Contribution from the Research Institute, The Hospital for Sick Children, Toronto, Canada, and the Department of Biochemistry, University of Toronto, Toronto, Canada

Equilibria and Structures of the Species in the Ternary System of L-Histidine, Copper(II), and Diglycyl-L-histidine, a Peptide Mimicking the Copper(II)-Transport Site of Human Serum Albumin

THEO P. A. KRUCK and BIBUDHENDRA SARKAR*

Received March 5, 1975 AIC501663

Diglycyl-L-histidine is a peptide molecule designed to mimic the specific Cu(II)-transport site of human albumin. The equilibria involved in the ternary system M–A–B (M = Cu(II), A = diglycyl-L-histidine, and B = L-histidine) have been investigated by analytical potentiometry in aqueous solution (0.15 *M* NaCl, 25°). The ternary system showed the presence of five mixed complexes (MH_2AB, MHAB, MAB, $MH_{-1}AB$, $MH_{-2}AB$) in addition to the binary complex species (MA, $MH_{-1}A$, $MH_{-2}A$, MHB, MB, MHB_2, MB_2). The species distribution and their stability constants were evaluated by the mathematical analysis of the potentiometric data. The species were further confirmed by their individual spectra computed from absorption measurements made on the total system. The combined results of the species distribution and visible spectra as well as those obtained from the proton displacement studies were utilized to propose the structures of the species in solution. From the analysis of the ternary complex data, it was possible to suggest structures for the mixed complexes existing at physiological pH. The structural features provide further evidence in support of the proposed role of L-histidine–Cu(II)–albumin in the physiological transportation of Cu(II).

Introduction

The design and synthesis of a peptide molecule[1-4] mimicking the specific Cu(II)-transport site of human serum albumin[5-9] provided an ideal opportunity to study in detail the nature of coordination equilibria existing in approximated physiological conditions. With a small molecule which is the simplification of the natural binding site sequence, it is possible to execute many important studies which are otherwise not feasible with a protein molecule. Human albumin is a physiologically important transport protein. Copper(II) bound to albumin is exchangeable and is known to be the transport form of Cu(II) in blood.[10,11] Sarkar and coworkers[12,13] had suggested that the ternary complex L-histidine–Cu(II)–albumin acts as an intermediate in the exchange of Cu(II) in blood between a macromolecule such as albumin and a low molecular weight substance like an amino acid.[14] Little is known, however, about the chemistry of mixed coordination by proteins. Since Cu(II) bound to the designed peptide diglycyl-L-histidine simulates many characteristics of Cu(II)–albumin,[4] the ternary system L-histidine–Cu(II)–diglycyl-L-histidine can be considered a representative of the ternary complex L-histidine–Cu(II)–albumin. We have reported detailed studies involving the binary and ternary coordination complexes of peptides[15,16] and amino acids[17-24] but no such investigations have yet been undertaken with a peptide having an imidazole side chain.

In the present communication, we have made a detailed investigation of the system L-histidine–Cu(II)–diglycyl-L-histidine in 0.15 *M* NaCl at 25°. The existing species were first detected by the mathematical analysis of potentiometric data. The stability constants of the species and their distributions were computed utilizing the technique of analytical potentiometry.[20] The species were confirmed by their different spectral characteristics. The individual spectrum was computed from absorption measurements made on the total system in conjunction with the previously calculated species distribution. Possible structures of the species are discussed on the basis of their proton displacement patterns and spectral characteristics. Results lend support to the proposed role[12,13] of the L-histidine–Cu(II)–albumin ternary complex in the transportation of Cu(II).

Experimental Section

Materials. Diglycyl-L-histidine was synthesized in our laboratory.[4] The purity was checked by thin-layer chromatography and by electrophoresis at different pH values. The concentration of the peptide was established by titration and by quantitative analysis with Pauly's reagent. L-Histidine free base ($[\alpha]^{20}D$ +39.9 ± 0.5°) was obtained from Nutritional Biochemicals. The puritiy was tested by chromatography. It was dried at 110° for 24 hr and then stored over anhydrous calcium chloride at room temperature under vacuum. All the reagents were of analytical grade.

Potentiometric Titration. The potentiometric titrations were performed on a Radiometer automatic titration assembly consisting of an expanded-scale pH meter, PHM26, an automatic titrator, TTT11B, an automatic recorder, SBRII, an automatic syringe, and a 50-ml thermostated titration assembly set to 25 ± 0.05°. The electrode train consisted of the Radiometer glass electrode, G202B, and the reference electrode, K401. The instrument was calibrated using three buffers [0.05 *m* tetraoxalate (pH 1.65 at 25°), 0.05 *m* phthalate (pH 4.008 at 25°), and 0.03 *m* phosphate (pH 7.415 at 25°)]. Argon was used throughout the titration to maintain an oxygen-free atmosphere. The water was first distilled and deionized by passing it through a commercial ion-exchange column (ILICO WAY-X research model). The base used for the titration was carbonate-free 1.0024 *N* NaOH which was standardized against primary standard potassium hydrogen phthalate obtained from the National Bureau of Standards. A CO_2-free atmosphere for the base was ensured at all times. A solution of 0.12 *N* HCl was prepared and was standardized against the calibrated NaOH. Stock solutions of $CuCl_2$ were prepared in 10^{-3} *M* HCl and calibrated titrimetrically.

Spectrophotometry. Absorbance measurements were made in cells having either 5- or 1-cm path lengths in a Cary 15 recording spectrophotometer thermostated at 25 ± 0.1°. All solutions for the spectral measurements were prepared in 0.15 *M* NaCl. The apparatus was aligned with 0.15 *M* NaCl in both reference and sample cells.

Results

Calculation of Results. The complexation reactions occurring between C_M moles of metal ion M, C_H moles of hydrogen ion H, C_A moles of ligand anion diglycyl-L-histidine, A, and C_B moles of ligand anion L-histidine, B, can be represented by the general equilibrium reaction

$$pM + qH + rA + sB \rightleftarrows M_pH_qA_rB_s \quad (1)$$

where p, q, r, and s are number of M, H, A, and B, respectively. The stabilities of the species formed are measured by the stoichiometric equilibrium constants β_{pqrs} expressed in terms of concentrations at constant ionic strength, temperature, and pressure

$$\beta_{pqrs} = [M_pH_qA_rB_s]/m^p h^q a^r b^s \quad (2)$$

where m, h, a, and b are the concentrations of free metal ion, hydrogen ion, ligand A, and ligand B. The following sets of

* To whom correspondence should be addressed at The Hospital for Sick Children.

Table I. Sample Compositions of the Ternary System M-A-B (M = Cu(II), A = Diglycyl-L-histidine, B = L-Histidine) Titrated in 0.15 *M* NaCl at 25°

Sample no.	$10^3C_M, M$	$10^3C_A, M$	$10^3C_B, M$
	Metal Variation		
1	0.828	3.430	3.996
2	1.656	3.430	3.996
3	2.484	3.430	3.996
	Ligand A Variation		
4	1.656	1.716	3.996
5	1.656	3.430	3.996
6	1.656	5.146	3.996
	Ligand B Variation		
7	1.656	3.430	0.798
8	1.656	3.430	1.998
9	1.656	3.430	3.996

equations define the total system

$$C_M = m + \Sigma p\beta_{pqrs} m^p h^q a^r b^s \quad (3)$$

$$C_H = h - oh + \Sigma q\beta_{pqrs} m^p h^q a^r b^s \quad (4)$$

$$C_A = a + \Sigma r\beta_{pqrs} m^p h^q a^r b^s \quad (5)$$

$$C_B = b + \Sigma s\beta_{pqrs} m^p h^q a^r b^s \quad (6)$$

where *oh* represents the amount of free hydroxyl ions. The experimental data and titration curves (−log $h = f$(base)) were obtained from solutions of defined concentrations of C_M, C_H, C_A, and C_B. The following relationships were used to obtain the values for the unbound portions of metal and the different ligands throughout the titration

$$pM = pM_0 + \int_{pH_0}^{pH_i} \frac{\delta H_1^+}{\delta C_M} dpH \quad (7)$$

$$pA = pA_0 + \int_{pH_0}^{pH_i} \frac{\delta H_1^+}{\delta C_A} dpH \quad (8)$$

$$pB = pB_0 + \int_{pH_0}^{pH_i} \frac{\delta H_1^+}{\delta C_B} dpH \quad (9)$$

where pM = −log [free metal M], pA = −log [free ligand A], pH = −log H, pB = −log [free ligand B], H_1^+ = moles of OH^- consumed to titrate hydrogen ions liberated through the complexation reactions. Subscript 0 denotes an initial known state of the system. The mathematical analyses of the data were performed by the sequential use of three computer programs,[20] using a GE 440 computer according to the method described by us earlier.[21]

Potentiometry. All solutions contained known amounts of HCl to lower the pH to such values that very little or no metal binding took place. The solutions were titrated with 1.0024 *N* NaOH. The concentrations of reactants in each sample are listed in Table I.

Proton–L-Histidine–Cu(II)–Diglycyl-L-histidine System. Solutions having the composition given in Table I were titrated, and the titration curves are given in Figure 1. The data were digitized and processed by program PLOT-2 to give the variations of pM, pA, and pB as a function of pH.

Species Distribution. The distribution of complexes is given in Figure 2 in terms of percent bound Cu(II) as a function of pH for a solution containing fixed amounts of C_M, C_A, and C_B in the approximate ratio of 1:2:2 ($C_M = 1.656 \times 10^{-3}$ *M*, $C_A = 3.430 \times 10^{-3}$ *M*, and $C_B = 3.996 \times 10^{-3}$ *M*). This provided at all times an excess of ligand in relation to the binding ability of the Cu(II) ion. The relative concentrations of the binary complex species were calculated, using the stability constants obtained in separate earlier experiments[4,23,24] and the values of unbound metal, unbound ligand A, or unbound ligand B determined in the present study. The remaining bound Cu(II) was assumed to be present in

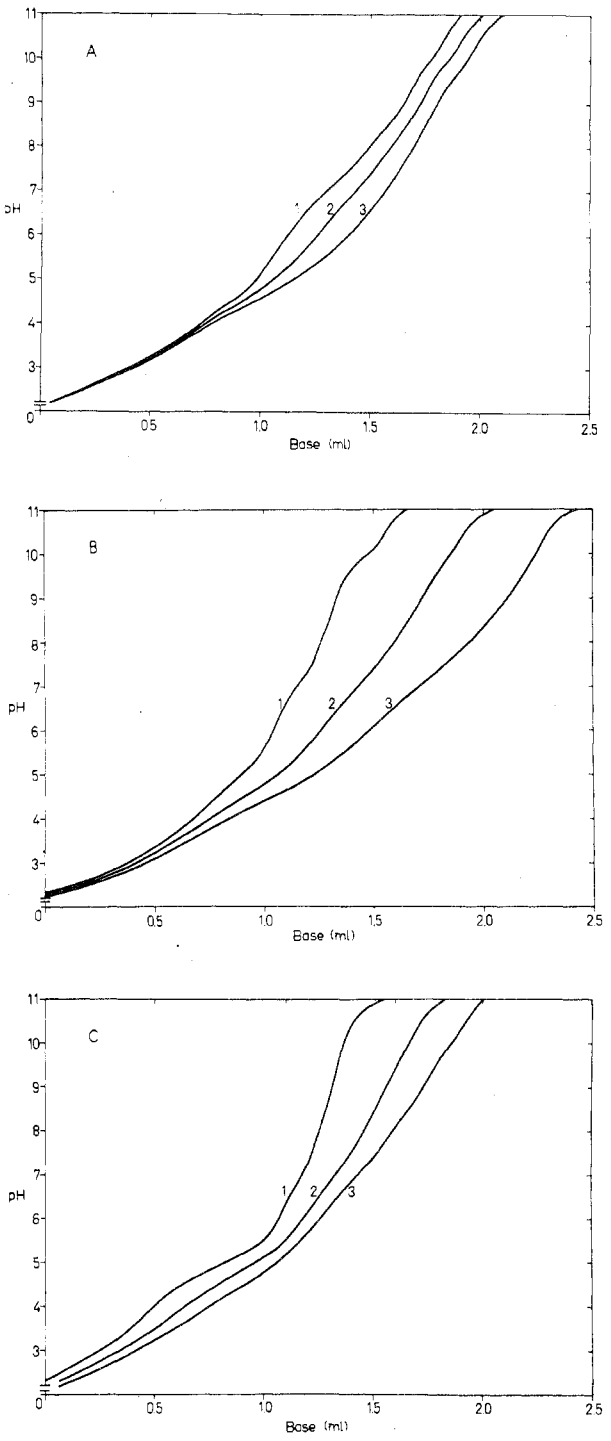

Figure 1. Titration curves for the system proton-L-histidine-Cu(II)-diglycyl-L-histidine. A. Metal variation: curve 1, $C_M = 0.828 \times 10^{-3}$ *M*, $C_A = 3.430 \times 10^{-3}$ *M*, $C_B = 3.996 \times 10^{-3}$ *M*; curve 2, $C_M = 1.656 \times 10^{-3}$ *M*, $C_A = 3.430 \times 10^{-3}$ *M*, $C_B = 3.996 \times 10^{-3}$ *M*; curve 3, $C_M = 2.484 \times 10^{-3}$ *M*, $C_A = 3.430 \times 10^{-3}$ *M*, $C_B = 3.996 \times 10^{-3}$ *M*. B. Ligand A variation: curve 1, $C_M = 1.656 \times 10^{-3}$ *M*, $C_A = 1.716 \times 10^{-3}$ *M*, $C_B = 3.996 \times 10^{-3}$ *M*; curve 2, $C_M = 1.656 \times 10^{-3}$ *M*, $C_A = 3.430 \times 10^{-3}$ *M*, $C_B = 3.996 \times 10^{-3}$ *M*; curve 3, $C_M = 1.656 \times 10^{-3}$ *M*, $C_A = 5.146 \times 10^{-3}$ *M*, $C_B = 3.996 \times 10^{-3}$ *M*. C. Ligand B variation: curve 1, $C_M = 1.656 \times 10^{-3}$ *M*, $C_A = 3.430 \times 10^{-3}$ *M*, $C_B = 0.798 \times 10^{-3}$ *M*; curve 2, $C_M = 1.656 \times 10^{-3}$ *M*, $C_A = 3.430 \times 10^{-3}$ *M*, $C_B = 1.998 \times 10^{-3}$ *M*; curve 3, $C_M = 1.656 \times 10^{-3}$ *M*, $C_A = 3.430 \times 10^{-3}$ *M*, $C_B = 3.996 \times 10^{-3}$ *M*.

ternary coordination complexes of the form $M_pH_qA_rB_s$. The test for probable species in this system employed the following

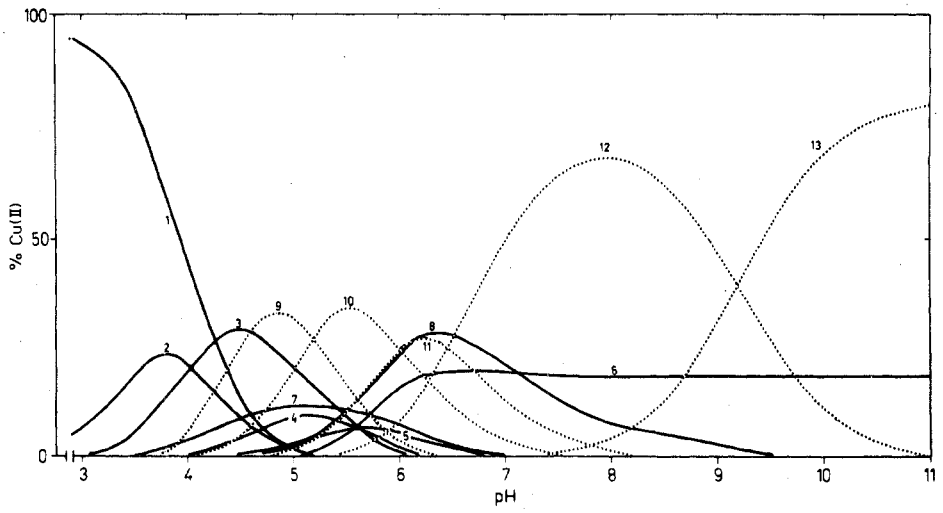

Figure 2. Species distribution in L-histidine–Cu(II)–diglycyl-L-histidine system as a function of pH: curve 1, unbound Cu(II); curve 2, MHB; curve 3, MB; curve 4, MA; curve 5, $MH_{-1}A$; curve 6, $MH_{-2}A$; curve 7, MHB_2; curve 8, MB_2; curve 9, MH_2AB; curve 10, MHAB; curve 11, MAB; curve 12, $MH_{-1}AB$; curve 13, $MH_{-2}AB$.

Table II. log Stability Constants (log β_{pqrs}) and the Standard Deviations ($\sigma(\log \beta_{pqrs})$) of the Ternary Complex Species $M_pH_qA_rB_s$ (M = Cu(II), A = Diglycyl-L-histidine, B = L-Histidine) Detected in the Ternary System in 0.15 *M* NaCl at 25°

p	*q*	*r*	*s*	log β_{pqrs}	$\sigma(\log \beta_{pqrs})$
1	2	1	1	28.83	0.019
1	1	1	1	23.61	0.017
1	0	1	1	17.56	0.010
1	−1	1	1	11.05	0.009
1	−2	1	1	1.7	0.008

values: $p = 1$; $q = +5, ..., 0, ..., -4$; $r = 1, 2$; $s = 1, 2$. Program GUESS-2 was used to locate the probable species along the pH scale. Calculations of the probable β_{pqrs} values for the complex species contained in the system were performed using program LEASK-2. The presence of a species was judged by its ability to reduce significantly the overall standard deviation of the least-squares fit. Only the series of protonated species listed in Table I was found to give satisfactory fit over the total pH range and, at the same time, it gave low standard deviations associated with the individual complex stability constants. It was not found necessary to employ more refined statistical methods for species selection since, with any other combination (p, q, r, s) tested, the errors increased greatly. Futhermore, polymer formation was excluded in a previous publication relating to the Cu(II)–diglycyl-L-histidine binary system.[4] The species found to be present in this system are MA, $MH_{-1}A$, $MH_{-2}A$, MHB, MB, MHB_2, MB_2, MH_2AB, MHAB, MAB, $MH_{-1}AB$, and $MH_{-2}AB$. The refined values for stability constants log β_{pqrs} are listed in Table II.

Spectrophotometry. Solutions containing C_M, C_A, and C_B in the ratio 1:2:2 were prepared under argon atmosphere for spectroscopic investigation. The pH was adjusted to various values covering a similar range (pH 3–11) as that being used for the studies of the species formation. At selected pH values, the spectra of the solutions were obtained in the visible region from 450 to 750 nm. The composition of the solution examined was similar to the one used for the calculation of the species distribution. The graphs are shown in Figure 3. If the Beer–Lambert law is obeyed by all the absorbing species contained in the complex mixture, then relation 10 will hold,

$$A_\lambda = \Sigma \epsilon_{\lambda,pqrs}[M_pH_qA_rB_s] \quad (10)$$

where A_λ is the total absorbance at wavelength λ, 1-cm light path, and ϵ_{pqrs} is the molar extinction of the species $M_pH_qA_rB_s$ at that wavelength.

The data shown in Figure 3 were processed to obtain the

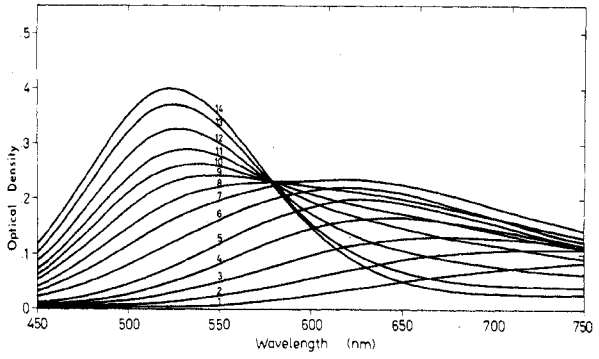

Figure 3. Optical absorption spectra observed on the L-histidine–Cu(II)–diglycyl-L-histidine system ($C_M = 2.034 \times 10^{-3}$ *M*, $C_A = 3.430 \times 10^{-3}$ *M*, $C_B = 3.996 \times 10^{-3}$ *M*), at various pH values: curve 1, pH 3.04; curve 2, pH 3.50; curve 3, pH 4.00; curve 4, pH 4.50; curve 5, pH 5.01; curve 6, pH 5.48; curve 7, pH 5.98; curve 8, pH 6.59; curve 9, pH 7.03; curve 10, pH 7.40; curve 11, pH 7.92; curve 12, pH 8.82; curve 13, pH 9.67; curve 14, pH 11.28.

absorbance A_λ as a function of pH (λ kept constant). These deduced functions are graphed in Figure 4. This was necessary in order to permit data processing according to eq 10. Each of these functions at constant λ represents an experimental vector A_λ which can be compared with a calculated vector A_λ'. The latter represents the sum total of each absorbing species. This contribution is, of course, the product between molar absorption and concentration as stated in eq 10. For each pH value, there are contributions by each species giving unique equations of the type shown in eq 10. Incremental steps of 0.2 pH unit were selected to set up the matrix of coefficients $[M_pH_qA_rB_s]$. Up to 20 equations were centered around the region where a particular species, whose $\epsilon_{\lambda,pqrs}$ was to be evaluated, was maximally present. At the same time, for such species where the $\epsilon_{\lambda,pqrs}$ had been determined previously in the binary system, these values were treated as constants. The remaining $\epsilon_{\lambda,pqrs}$'s were treated as unknowns. These sets of simultaneous equations were solved by program LEASK-2. The resulting solution vector represents the individual absorption contributions due to each complex species. This calculation was repeated for the wavelength covering the region λ 460–680 nm in increments of 20 nm. The components $\epsilon_{\lambda,pqrs}$ of each solution vector are plotted as functions of wavelength λ to give the graphs shown in Figure 5. From the peak region of each absorbing species the corresponding ϵ_{max} and λ_{max} were evaluated and are listed in Table III.

Analyses of Proton Displacement Data for Structural In-

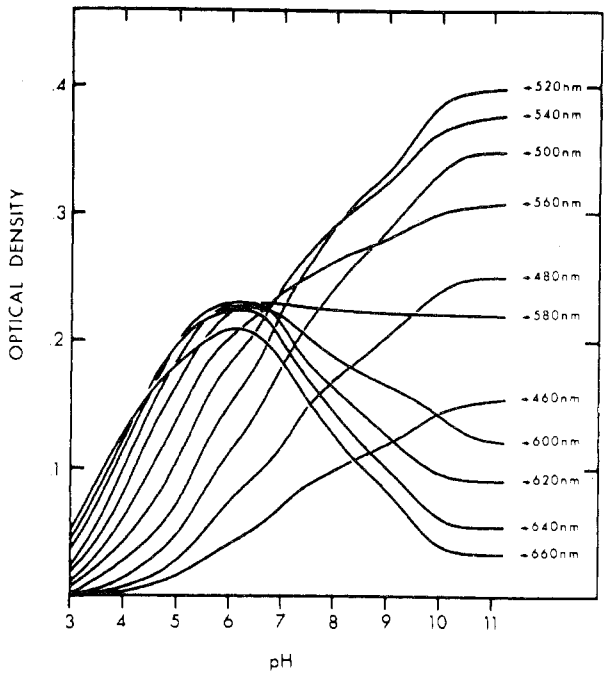

Figure 4. Optical absorption spectra of aqueous L-histidine-Cu(II)-diglycyl-L-histidine solutions at constant wavelength (as marked on the graphs) plotted as functions of pH.

Table III. Maximum Values of Extinction Coefficients (ϵ_{max}) and Corresponding Wavelength (λ_{max}) of Complexes $M_pH_qA_rB_s$ (M = Cu(II), A = Diglycyl-L-histidine, B = L-Histidine)

Species $M_pH_qA_rB_s$				ϵ_{max},	
p	q	r	s	M^{-1} cm^{-1}	λ_{max}, nm
1	2	1	1	113	620
1	1	1	1	110	570
1	0	1	1	79	630
1	−1	1	1	76	535
1	−2	1	1	103	515
1	−2	1	1	103	525
1	1	0	1[a]	65	750
1	0	0	1[a]	45	670
1	0	0	2[a]	86	640

[a] Taken from ref 24.

terpretation. Earlier studies have shown that the analyses of the proton displacement data for structural elucidation can be very useful in studying metal–ligand interaction.[24] The proton displacement data for the ternary system are given in Figure 6. The graphs show the proton liberation due to metal addition (Figure 6, curve 1), peptide addition (Figure 6, curve 2), and L-histidine addition (Figure 6, curve 3), where, in the case of the variation of any one component, all the others were kept constant. Ligands in the ternary system have well-separated pK_a values of the individual protonated groups. It should be noted that the total proton liberation at a given pH must equal the contributions of each species yielding protons

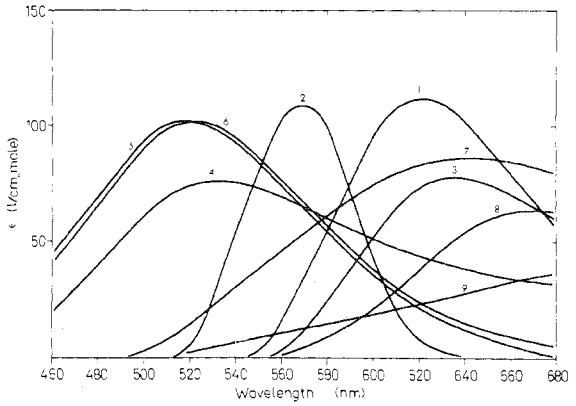

Figure 5. Computed spectra of the species in the L-histidine-Cu(II)-diglycyl-L-histidine system: curve 1, MH_2AB; curve 2, MHAB; curve 3, MAB; curve 4, $MH_{-1}AB$; curve 5, $MH_{-2}AB$; curve 6, $MH_{-2}A$; curve 7, MB_2; curve 8, MB; curve 9, MHB.

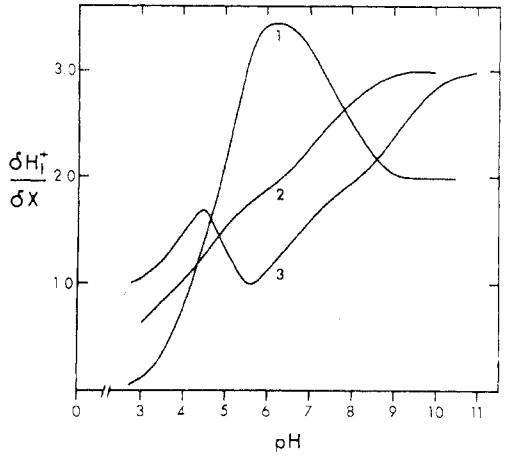

Figure 6. Proton displacement as a function of pH for the L-histidine-Cu(II)-diglycyl-L-histidine system ($C_M = 1.656 \times 10^{-3}$ M, $C_A = 3.430 \times 10^{-3}$ M, $C_B = 3.996 \times 10^{-3}$ M): curve 1, $\partial H_1^+/\partial C_M$; curve 2, $\partial H_1^+/\partial C_A$; curve 3, $\partial H_1^+/\partial C_B$.

when the metal–ligand bonds are formed. For the theoretical calculations of proton displacement, it is necessary to consider all the species in the system. For the purpose of computation it is also necessary to take into account all the possible modes of binding. The scheme in Table IV shows the permutations for the possible modes of coordination in the complex species $MH_{-2}AB$, $MH_{-1}AB$, and $MH_{-2}A$ existing in the pH region 8–11. Utilizing the concentration of species at a given pH (Figure 2) and the pK_a values of the probable groups involved in binding, the theoretical proton liberation data $\partial H_1^+/\partial C_M$ at various pH values were calculated. These calculations were performed by program SELECT[24] which compared the observed data (Figure 6) with the theoretical values according to the scheme outlined in Table IV. The deviations between these two sets of data are listed in Table V. The least deviation

Table IV. Scheme for Proton Displacement Calculations for the Ternary System (pH 8–11)

Coordination pattern[a]	No. of potential groups involved in coordination[b]												
	$MH_{-2}AB$					$MH_{-1}AB$					$MH_{-2}A$		
	A			B		A			B		A[c]		
	N_{im}	NH_2	N_{pep}	N_{im}	NH_2	N_{im}	NH_2	N_{pep}	N_{im}	NH_2	N_{im}	NH_2	N_{pep}
I	1	1	2	1	0	1	1	2	1	0	1	1	2
II	0	1	2	1	0	0	1	2	1	0	1	1	2
III	0	1	2	0	1	0	1	2	0	1	1	1	2

[a] There are other possible combinations, but no reasonable fit could be obtained. [b] The numerals indicate the number of protons which can be released upon metal coordination with the particular group listed. [c] Since the structure of $MH_{-2}A$ is well characterized[4], patterns I, II, and III are kept identical.

Table V. Difference between the Calculated and Observed Proton Displacement Data for Structure Analysis

No.	Coordination pattern MH_{-2}-AB	MH_{-1}-AB	MH_{-2}-A	H_1^+(calcd) − H_1^+(obsd) pH 11.00	pH 10.00	pH 9.75	pH 9.50	pH 9.25	pH 9.00	pH 8.75	pH 8.50	pH 8.25	pH 8.00
1	I	I	I	−0.01	0.01	−0.04	−0.04	−0.03	−0.07	0.04	−0.05	−0.09	−0.09
2	I	II	I	−0.01	0.02	−0.01	0.04	0.13	0.10	0.11	0.04	−0.03	−0.06
3	III	I	I	0.00	0.10	0.08	0.11	0.15	0.20	0.35	0.44	0.49	0.53
4	III	III	I	0.00	0.11	0.11	0.19	0.30	0.37	0.49	0.54	0.55	0.57

in a particular combination was considered to be the closest fit.

Discussion

The formation of a series of mixed complexes, in addition to several binary species of varying states of protonation, has been observed in the ternary system. They are of the form MH_2AB, MHAB, MAB, $MH_{-1}AB$, and $MH_{-2}AB$. A complete analysis of the equilibria should be considered a prerequisite to study the structure of the species in solution in a multispecies system. From the total stoichiometric formulas for these protonated complexes it is not possible to predict which groups on either ligand molecule are coordinated to the central Cu(II) ion. However, when the species distribution, the proton liberation data, and the calculated optical spectra are considered simultaneously, then it is possible to obtain valuable information about the structural features of the complex species involved.

The species distribution in Figure 2 does not show any region where there is one complex species existing exclusively. Therefore, the proton liberation data, $\partial H_1^+/\partial C_M$, were processed for a selected region (pH 8–11) where a minimum of overlapping complex $MH_{-2}A$ and two ternary complexes $MH_{-1}AB$ and $MH_{-2}AB$ exist simultaneously. The proton displacement data listed in Table V (line 1) showed a minimum deviation between the calculated and the observed values. Hence, we can accept the coordination pattern I, I, I set out in Table IV as representative of the type of coordination exhibited by the complexes examined. The coordination pattern of $MH_{-2}A$ has been established in the binary system earlier[4] and the analysis of the ternary system data confirms its proposed structure (Figure 7A). Both mixed-complex species $MH_{-2}AB$ and $MH_{-1}AB$ require on the part of the peptide moiety the involvement of two peptide amide nitrogens and the amino group of the peptide. In the L-histidine moiety of these mixed complexes, only the amino group carries a proton in the pH region studied. The proton displacement analysis as outlined in the scheme listed in Table IV and the results listed in Table V show that in the complex $MH_{-1}AB$, the L-histidine amino group cannot be involved in Cu(II) coordination. However, at pH >3 all Cu(II)–L-histidine complexes show at least bidentate or even tridentate metal–ligand coordination involving the carboxyl group and either the amino or the imidazole group or both.[24] At the same time, no evidence could be found in the literature where, at neutral or higher pH values, there was monodentate attachment of the carboxyl group of L-histidine to the Cu(II) ion. Consequently, if the amino group is not involved in $MH_{-1}AB$, then the imidazole group of L-histidine is the most likely group coordinating to Cu(II) in the fourth position of the coordination plane. The observed λ_{max} 535 nm is consistent with the presence of an amino nitrogen, two peptide nitrogens, and an imidazole nitrogen in the coordination plane of the Cu(II) ion.[26,27] Also, it has been shown by Freeman et al.[25] that the carboxyl group of L-histidine in a ternary complex can coordinate in an axial position in the coordination sphere of the central Cu(II) ion. Therefore, it is reasonable to suggest that the L-histidine moiety in the $MH_{-1}AB$ complex is probably coordinated via its imidazole and carboxyl group as shown in Figure 7B.

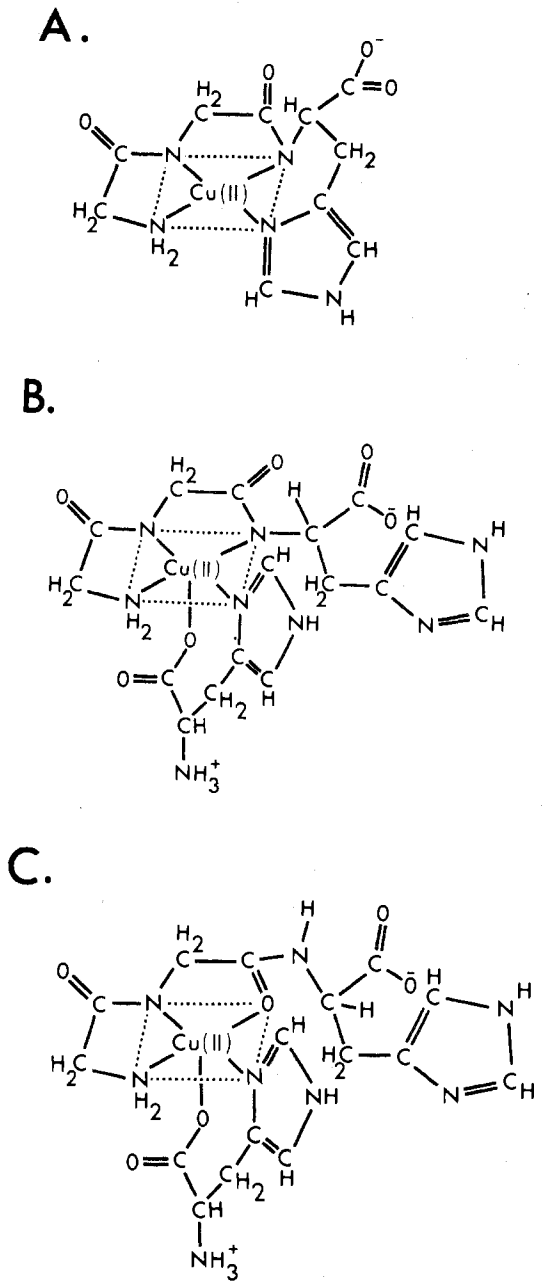

Figure 7. Proposed structures of species in the L-histidine–Cu(II)–diglycyl-L-histidine system: A, $MH_{-2}A$; B, $MH_{-1}AB$; C, MAB.

Upon raising the pH from 8 to 10, we see the transition (Figure 2) from the species $MH_{-1}AB$ to the species $MH_{-2}AB$. This transition parallels the proton loss from the amino group of L-histidine due to its inherent pK_a. The L-histidine moiety is the only group capable of dissociating a proton (in the pH region cited) in order to form the species $MH_{-2}AB$. Lowering of the pK_a is indicative of metal coordination. Inspection of Figure 6, curve 3, reveals that in the pH region 8–11 there is no indication of a lowering of the $pK_{NH_3^+}$ of L-histidine. Therefore, it is likely that the amino group of the L-histidine

moiety of the mixed complex is not involved in Cu(II) coordination. Since, according to the proton liberation analysis, the coordination pattern of the peptide moiety does not change going from complex $MH_{-1}AB$ to $MH_{-2}AB$, one can safely attribute the change in protonation state to the loss of a proton from the amino group of L-histidine in the ternary complex. The small change in λ_{max} from 535 nm for $MH_{-1}AB$ to 515 nm for $MH_{-2}AB$ we relate to the alteration in the charge distribution due to the loss of a proton from the complex. A likely structure for this species would be the same as Figure 7B, except that it has lost a proton from the amino group of L-histidine.

Below pH 8 the species distribution becomes very complex. The spectral results show a large shift of λ_{max} from 535 nm for $MH_{-1}AB$ to 630 nm for MAB. This is indicative of a rearrangement of the ligands positioned in the coordination square of the Cu(II) ion. If the amide nitrogens are still coordinated to Cu(II), besides the α-NH_2 nitrogen, then a λ_{max} <600 nm should be observed. Work done by Hartzell and Gurd[26] and Bryce and Gurd[27] shows the relationship of resulting visible light absorption as a function of coordination bonds involved in Cu(II)–peptide complexes. Characteristic absorption bands have been established for complex species in which the α-NH_2 and subsequent peptide nitrogens are involved: α-NH_2 + 1 peptide amide nitrogen, λ_{max} 660 nm; α-NH_2 + 2 peptide amide nitrogens, λ_{max} 575 nm; α-NH_2 + 3 peptide amide nitrogens, λ_{max} 515 nm.[26,27] Accordingly, if we had Cu(II)–peptide only, we would invoke α-NH_2 and two peptide amide nitrogens. However, in the ternary complex, the third coordination position can be occupied by the second peptide amide nitrogen or by its corresponding carbonyl oxygen. The latter type of coordination to Cu(II) has been discussed earlier by Martin, Mosoni, and Sarkar[16] with the ternary complex glycine–Cu(II)–diglycylglycine. The L-histidine in this ternary complex can bind the Cu(II) with its imidazole in the square plane and carboxyl group in an axial position. The structure envisaged for MAB is shown in Figure 7C. A similar structure for this species was proposed in association with kinetic observations.[28] Another arrangement of the ligands is also possible, which would satisfy both the stoichiometric proton balance and the spectral data, involving L-histidine in a tridentate coordination and the peptide molecule being bound through its α-NH_2 group and its first carbonyl oxygen. However, the kinetic results[28] reported on the same system do not support this structure. With decreasing pH values, the next two complexes appear in sequence MHAB and MH_2AB with the spectra changing from 630 nm for MAB to λ_{max} 570 nm and to λ_{max} 620 nm, respectively. This again indicates a successive rearrangement of the ligands around the Cu(II) ion. The proton liberation curve in Figure 6, curve 3, shows an interesting feature. Upon increasing the pH above 4.5, there occurs a decreasing amount of proton liberation. This decrease can be attributed to proton consumption occurring as a consequence of L-histidine forming coordination bonds with Cu(II)–diglycyl-L-histidine molecules. As the Cu(II)–L-histidine coordination bonds are formed, certain groups of the peptide get displaced. These newly released groups having pK_a values above the pH of observation will consume protons, the result being as shown in Figure 6, curve 3. At this time, sufficient evidence is lacking to enable one to distinguish between several possible structures for these species.

There may be some important biological significance of the extensive rearrangements of the mixed complex L-histidine–Cu(II)–diglycyl-L-histidine taking place in the form of various species around the neutral pH. Diglycyl-L-histidine was designed to mimic the specific Cu(II) binding site of albumin[1,2] and it has been demonstrated that this peptide molecule does bind Cu(II) in a similar fashion as it does to albumin.[3,4] By analogy, L-histidine–Cu(II)–diglycyl-L-histidine is representative of L-histidine–Cu(II)–albumin. This protein ternary complex was detected earlier and a role was proposed.[12,13] If the ternary complex were a rigid structure with a low ligand-exchange rate, then it would be unsuitable for transport mechanism. However, it appears that the complexes can rearrange with great facility. This process of steric rearrangement may, in fact, enhance the ligand-exchange rates, thus making the ternary complex amino acid–Cu(II)–albumin an ideal intermediate for the transfer of Cu(II) between albumin and amino acid.

Acknowledgment. This work was supported by the Medical Research Council of Canada.

Registry No. L-Histidine, 71-00-1; diglycyl-L-histidine, 7451-76-5; Cu, 7440-50-8; $MH_{-2}A$, 53554-01-1; $MH_{-1}AB$, 55853-41-3; $MH_{-2}AB$, 55853-42-4; MAB, 55853-43-5.

References and Notes

(1) B. Sarkar, *Proc. Can. Fed. Biol. Soc.*, **15**, 659 (1972).
(2) B. Sarkar, *Proc. Int. Congr. Biochem.*, **9**, 122 (1973).
(3) B. Sarkar, T. P. A. Kruck, and S. Lau, *Proc. Int. Conf. Coord. Chem.*, **15**, 472 (1973).
(4) S. Lau, T. P. A. Kruck, and B. Sarkar, *J. Biol. Chem.*, 249, 5878 (1974).
(5) T. Peters, Jr., and F. A. Blumenstock, *J. Biol. Chem.*, **242**, 1574 (1967).
(6) R. A. Bradshaw and T. Peters, Jr., *J. Biol. Chem.*, **244**, 5582 (1969).
(7) W. T. Shearer, R. A. Bradshaw, F. R. N. Gurd, and T. Peters, Jr., *J. Biol. Chem.*, **242**, 5451 (1967).
(8) E. Breslow, *J. Biol. Chem.*, **239**, 2352 (1964).
(9) R. A. Bradshaw, W. T. Shearer, and F. R. N. Gurd, *J. Biol. Chem.*, **243**, 3817 (1968).
(10) A. G. Bearn and H. G. Kunkel, *Proc. Soc. Exp. Biol. Med.*, **88**, 44 (1954).
(11) P. Z. Neumann and A. Sass-Kortsak, *J. Clin. Invest.*, **46**, 646 (1967).
(12) B. Sarkar and Y. Wigfield, *Can. J. Biochem.*, **46**, 601 (1968).
(13) S. Lau and B. Sarkar, *J. Biol. Chem.*, **246**, 5938 (1971).
(14) B. Sarkar and T. P. A. Kruck, "Biochemistry of Copper", J. Peisach, P. Aisen, and W. E. Blumberg, Ed., Academic Press, New York, N.Y., 1966, p 183.
(15) B. Sarkar, M. L. Lee, and R.-P. Martin, *Proc. Can. Fed. Biol. Soc.*, **12**, 14 (1969).
(16) R.-P. Martin, L. Mosoni, and B. Sarkar, *J. Biol. Chem.*, **246**, 5944 (1971).
(17) B. Sarkar and T. P. A. Kruck, *Can. J. Biochem.*, **45**, 2046 (1967).
(18) B. Sarkar, M. Bersohn, Y. Wigfield, and T.-C. Chiang, *Can. J. Biochem.*, **46**, 596 (1968).
(19) B. Sarkar and T. P. A. Kruck, *Proc. Int. Conf. Coord. Chem.*, **14**, 193 (1972).
(20) The earlier versions of Programs PLOT, GUESS, and LEASK have been revised and modified to permit more efficient operation. These programs (PLOT-2, GUESS-2, and LEASK-2) are available in both Fortran-IV and APL languages. All inquiries regarding these programs should be directed to the corresponding author.
(21) B. Sarkar and T. P. A. Kruck, *Can. J. Chem.*, **51**, 3541 (1973).
(22) T. P. A. Kruck and B. Sarkar, *Can. J. Chem.*, **51**, 3549 (1973).
(23) T. P. A. Kruck and B. Sarkar, *Can. J. Chem.*, **51**, 3555 (1973).
(24) T. P. A. Kruck and B. Sarkar, *Can. J. Chem.*, **51**, 3563 (1973).
(25) H. C. Freeman, J. M. Guss, M. J. Healy, R.-P. Martin, C. E. Nocholds, and B. Sarkar, *Chem. Commun.*, 225 (1969).
(26) C. R. Hartzell and F. R. N. Gurd, *J. Biol. Chem.*, **244**, 147 (1969).
(27) G. F. Bryce and F. R. N. Gurd, *J. Biol. Chem.*, **241**, 122 (1966).
(28) S. Lau and B. Sarkar, *Can. J. Chem.*, **53**, 710 (1975).